Tracking and Therapeutic Value of Human Adipose Tissue–derived Mesenchymal Stem Cell Transplantation in Reducing Venous Neointimal Hyperplasia Associated with Arteriovenous Fistula[1]

Binxia Yang, MD, PhD
Akshaar Brahmbhatt, BS
Evelyn Nieves Torres, PhD
Brian Thielen
Deborah L. McCall, MS
Sean Engel
Aditya Bansal, PhD
Mukesh K. Pandey, PhD
Allan B. Dietz, PhD
Edward B. Leof, PhD
Timothy R. DeGrado, PhD
Debabrata Mukhopadhyay, PhD
Sanjay Misra, MD

Purpose: To determine if adventitial transplantation of human adipose tissue–derived mesenchymal stem cells (MSCs) to the outflow vein of B6.Cg-*Foxn1*^{nu}/J mice with arteriovenous fistula (AVF) at the time of creation would reduce monocyte chemoattractant protein-1 *(Mcp-1)* gene expression and venous neointimal hyperplasia. The second aim was to track transplanted zirconium 89 (^{89}Zr)–labeled MSCs serially with positron emission tomography (PET) for 21 days.

Materials and Methods: All animal experiments were performed according to protocols approved by the institutional animal care and use committee. Fifty B6.Cg-*Foxn1*^{nu}/J mice were used to accomplish the study aims. Green fluorescent protein was used to stably label 2.5×10^5 MSCs, which were injected into the adventitia of the outflow vein at the time of AVF creation in the MSC group. Eleven mice died after AVF placement. Animals were sacrificed on day 7 after AVF placement for real-time polymerase chain reaction ($n = 6$ for MSC and control groups) and histomorphometric ($n = 6$ for MSC and control groups) analyses and on day 21 for histomorphometric analysis only ($n = 6$ for MSC and control groups). In a separate group of experiments ($n = 3$), animals with transplanted ^{89}Zr-labeled MSCs were serially imaged with PET for 3 weeks. Multiple comparisons were performed with two-way analysis of variance, followed by the Student *t* test with post hoc Bonferroni correction.

Results: In vessels with transplanted MSCs compared with control vessels, there was a significant decrease in *Mcp-1* gene expression (day 7: mean reduction, 62%; $P = .029$), with a significant increase in the mean lumen vessel area (day 7: mean increase, 176% [$P = .013$]; day 21: mean increase, 415% [$P = .011$]). Moreover, this was accompanied by a significant decrease in Ki-67 index (proliferation on day 7: mean reduction, 81% [$P = .0003$]; proliferation on day 21: mean reduction, 60%, [$P = .016$]). Prolonged retention of MSCs at the adventitia was evidenced by serial PET images of ^{89}Zr-labeled cells.

Conclusion: Adventitial transplantation of MSCs decreases *Mcp-1* gene expression, accompanied by a reduction in venous neointimal hyperplasia.

Online supplemental material is available for this article.

[1] From the Vascular and Interventional Radiology Translational Laboratory, Department of Radiology (B.Y., A. Brahmbhatt, E.N.T., B.T., D.L.M., S.E., A. Bansal, M.K.P., T.R.D., S.M.), and Department of Biochemistry and Molecular Biology (A.B.D., E.B.L., D.M., S.M.), Mayo Clinic, 200 First St SW, Rochester, MN 55905. Received April 27, 2015; revision requested June 12; revision received July 20; accepted August 6; final version accepted September 14. A. Brahmbhatt was supported by the Howard Hughes Medical Institute (HHMI-SIRF 2013). **Address correspondence to** S.M. (e-mail: *misra.sanjay@mayo.edu*).

In the United States, more than 570 000 patients have end-stage renal disease, and most patients require hemodialysis for the purification of their blood (1). Optimally functioning hemodialysis vascular access is required so that patients may undergo purification of their blood and removal of electrolytes. The preferred location for hemodialysis vascular access is the arteriovenous fistula (AVF), and less than two-thirds of patients have a well-functioning AVF 1 year after the start of hemodialysis. In most patients, the AVF will fail because of venous neointimal hyperplasia (VNH) and venous stenosis formation (2,3).

There are many factors thought to contribute to the formation of VNH, including hypoxia, shear stress, oxidative stress, and inflammation (4). It is hypothesized that these factors result in elaboration of proinflammatory cytokines, including monocyte chemoattractant protein–1 (MCP-1), and others (5–7). As a consequence, this leads to accumulation of macrophages, leukocytes, and smooth-muscle cells, as identified with histologic analysis of specimens removed from a venous stenosis (8).

Mesenchymal stem cells (MSCs) have been isolated and expanded from several different sources, including bone marrow, adipose tissue, and cord blood (9). These cells have anti-inflammatory properties that can result in homeostasis, repair, and regeneration in pathologic responses caused by vascular injury (10). In other studies, investigators have demonstrated that MSC transplantation can reduce fibrosis in the heart, lung, liver, and kidney in experimental animal models (11–16). Along with having anti-inflammatory properties, MSCs can inhibit the proliferative effects of monocytes, tumor cells, and cardiac fibroblasts (17–20). Finally, MSCs have been shown to reduce hypoxic injury after myocardial infarction because they home to regions of hypoxia (21,22). In animal models of AVF or graft failure and in clinical specimens, increased expression levels of hypoxia-inducible factor–1α (HIF-1α) have been observed. Because of these different properties, MSCs have generated interest for the potential application of alleviating vascular injury. We used human adipose tissue–derived MSCs that were manufactured with good manufacturing practice and that are currently being used in several clinical trials at our institution.

Taken collectively, we hypothesized that adventitial transplantation of MSCs to the outflow vein of the AVF at the time of creation would reduce proinflammatory cytokines, including *Mcp-1,* thereby reducing VNH formation (23,24). The purpose of this study was to determine if adventitial transplantation of human adipose tissue–derived MSCs to the outflow vein of B6.Cg-*Foxn1*^{nu}/J mice with AVF at the time of creation would reduce *Mcp-1* gene expression and VNH. The second aim was to track transplanted zirconium 89 (^{89}Zr)–labeled MSCs serially by means of positron emission tomography (PET) imaging for 21 days.

Advances in Knowledge

- In vessels with transplanted mesenchymal stem cells (MSCs) compared with control vessels, there was a significant decrease in monocyte chemoattractant protein-1 gene expression (day 7: mean reduction, 62%; $P = .029$), with a significant increase in the mean lumen vessel area (day 7: mean increase, 176% [$P = .013$]; day 21: mean increase, 415% [$P = .011$]) and a significant decrease in the mean neointimal area and the medial and adventitial area (day 21: mean reduction, 77%; $P = .013$) and in neointimal cell density (day 7: mean reduction, 83% [$P = .0007$]; day 21: mean reduction, 83% [$P < .0001$]).
- This was accompanied by a significant decrease in Ki-67 index (proliferation on day 7: mean reduction, 81% [$P = .0003$]; proliferation on day 21: mean reduction, 60% [$P = .016$]), fibroblasts (day 7: mean reduction, 65% [$P = .0003$]; day 21: mean reduction, 42% [$P = .0016$]), smooth muscle cells (day 21: mean reduction, 27%; $P = .013$), and macrophage staining (day 7: mean reduction, 51%; $P = .033$), with a significant increase in cellular apoptosis (day 7: mean increase, 3061% [$P < .0001$]; day 21: mean increase, 425% [$P < .0001$]) when compared with controls.
- We were able to track transplanted zirconium 89–labeled MSCs with PET imaging for 21 days.

Implication for Patient Care

- Adipose tissue–derived MSC transplantation to the adventitia of the outflow vein of arteriovenous fistula may potentially help reduce venous stenosis formation.

Published online before print
10.1148/radiol.2015150947 **Content codes:** NM MI

Radiology 2016; 279:513–522

Abbreviations:
α-SMA = α–smooth-muscle actin
AVF = arteriovenous fistula
FSP-1 = fibroblast specific protein–1
GFP = green fluorescent protein
HIF-1α = hypoxia-inducible factor–1α
MSC = mesenchymal stem cell
TUNEL = terminal deoxynucleotidyl transferase dUTP nick end labeling
VNH = venous neointimal hyperplasia

Author contributions:
Guarantors of integrity of entire study, B.Y., S.M.; study concepts/study design or data acquisition or data analysis/interpretation, all authors; manuscript drafting or manuscript revision for important intellectual content, all authors; approval of final version of submitted manuscript, all authors; agrees to ensure any questions related to the work are appropriately resolved, all authors; literature research, A. Brahmbhatt, B.Y., D.L.M., A. Bansal, M.K.P., S.M.; clinical studies, S.M.; experimental studies, B.Y., A. Brahmbhatt, E.N.T., B.T., D.L.M., S.E., A. Bansal, M.K.P., A.B.D., T.R.D., S.M.; statistical analysis, B.Y., S.E., A. Bansal, S.M.; and manuscript editing, A. Bansal, M.K.P., T.R.D., D.M., S.M.

Funding:
This research was supported by the National Institutes of Health (grant HL098967).

Conflicts of interest are listed at the end of this article.

Materials and Methods

A.B.D. is an inventor of technology and has a leadership position within the company that supplies technology for growing MSCs used in this study. He did not have access to the data. T.R.D., M.K.P., and A. Bansal have a patent pending on ^{89}Zr labeling of cells. S.M. and A.B.D. have a patent pending on using MSCs for preventing stenosis formation in hemodialysis vascular access. The data were under the control of and analyzed by B.Y., A. Brahmbhatt, E.N.T., D.L.M., S.E., A. Bansal, M.K.P., T.R.D., and S.M.

Experimental Animals

All animal experiments were performed according to protocols approved by our institutional animal care and use committee. Housing and handling of the animals was performed in accordance with the Public Health Service Policy on Humane Care and Use of Laboratory Animals, which was revised in 2000. Animals were housed at 22°C temperature, 41% relative humidity, and 12-hour light-dark cycles. Animals were allowed access to water and food ad libitum. Fifty B6.Cg-*Foxn1*^{nu}/J mice weighing 20–25 g and aged approximately 6–8 weeks were purchased from Charles River Laboratories, Wilmington, Mass. These animals lack a thymus, are unable to produce T cells, and are therefore immunodeficient, which is ideal for xenograft research. Anesthesia was achieved with intraperitoneal injection of a mixture of ketamine hydrochloride (0.1–0.2 mg per gram of body weight) and xylazine (0.02 mg per gram of body weight). AVF between the right carotid artery and the ipsilateral jugular vein was created, as described previously (25). Green fluorescent protein (GFP) was used to stably label 2.5×10^5 MSCs in 5 μL of medium, which was injected into the adventitia of the outflow vein at the time of AVF creation in the MSC group. The 2×10^5 MSCs labeled with GFP were injected into the adventitia of the outflow vein at the time of AVF creation (Fig E1 [online]). Eleven mice died after cell transplantation. Animals were sacrificed on day 7 for either histomorphometric or real-time polymerase chain reaction analyses for each of the following groups: AVF only (control group, $n = 6$) and MSC (MSC group, $n = 6$). Another group of animals was sacrificed at day 21 after fistula placement for histomorphometric and immunohistochemical analyses for the following groups: AVF only (control group, $n = 6$) and MSC ($n = 6$, Fig E2 [online]). In a separate group of experiments, three mice were used for tracking Zr^{89}-labeled MSCs, and three mice had free Zr^{89} administered to the adventitia of the outflow vein after creation of an AVF.

Human MSC Preparation

Human MSCs from healthy donors were obtained from the Human Cellular Therapy Laboratory, Mayo Clinic, Rochester, Minn. These cells have been characterized with respect to surface markers and described elsewhere (26). Briefly, they are CD73(+), CD90(+), CD105(+), CD44(+), and HLA-ABC(+), and they are being used in several clinical trials.

GFP Transfection

MSCs were transfected with GFP lentivirus from Mayo Clinic Rochester Labs, Rochester, Minn. MSCs were grown overnight in media containing the GFP lentivirus. The medium was changed to complete growth medium the next day, and cells were checked for fluorescence after 48 hours. Once fluorescence was confirmed, the cells were cultured in complete media that contained 1 μg puromycin per milliliter. Cells containing the plasmid were expanded in complete growth media.

^{89}Zr Labeling and in Vivo Tracking of Stem Cells

Noninvasive PET imaging was used to evaluate the biodistribution of MSCs delivered to the adventitia outside the AVF in CD1-*Foxn1nu* mice. For this, MSCs were labeled with a biostable radiolabeling synthon, ^{89}Zr-desferrioxamine-N-chlorosuccinimide, as described previously (27). After delivery of 2×10^5 ^{89}Zr-labeled MSCs (at a radioactivity concentration of approximately 0.55 MBq per 10^6 cells) into the adventitia, the ^{89}Zr-labeled MSCs were tracked for 3 weeks by using a small-animal PET/radiography system (Genesys4; Sofie BioSystems, Culver City, Calif). In the control group, 0.28 MBq of ^{89}Zr $(HPO_4)_2$ was delivered into the adventitia. PET images were normalized to units of standardized uptake value, which was calculated as follows: tissue radioactivity concentration/(injected dose/body weight in grams).

Immunohistochemistry and Morphometric Analysis

After fixation with formalin and processing, the samples were embedded in paraffin. Histologic sectioning began at the outflow vein segment. Routinely, 80–120 5-μm sections were obtained, and the cuff used to make the anastomosis could be visualized. Every 25 μm, two to four sections were stained with hematoxylin-eosin, Ki-67, α–smooth-muscle actin (α-SMA), HIF-1α, CD68, fibroblast specific protein–1 (FSP-1), or terminal deoxynucleotidyl transferase dUTP nick end labeling (TUNEL) on paraffin-embedded sections from the outflow vein. The EnVision (Dako, Carpinteria, Calif) method was used with a heat-induced antigen retrieval step (28). The following antibodies were used: mouse monoclonal antibody Ki-67 (Dako, 1:400) or rabbit polyclonal antibody for CD68, α-SMA, FSP-1, and HIF-1α (Abcam, Cambridge, Mass; 1:600). Immunoglobulin G antibody staining was performed to serve as the control. Sections immunostained with hematoxylin-eosin, Ki-67, α-SMA, HIF-1α, CD68, FSP-1, or TUNEL were viewed by using an Axioplan 2 microscope (Zeiss, Oberkochen, Germany) equipped with a Neo-Fluor ×20/0.50 objective and digitized to capture a minimum of 1030 × 1300 pixels by using an Axiocam camera (Zeiss). Images were obtained that included the entire cross-section of the venous anastomosis by using KS 400 Image Analysis software (Zeiss). Ki-67, HIF-1α, or TUNEL-positive nuclei (brown) and total nuclei (brown and blue) were highlighted, in turn, by selecting the appropriate red-green-blue color intensity

range and were then counted. The color intensity was adjusted for each section to account for the decreasing intensity of positive staining over time. The Ki-67, HIF-1α, or TUNEL indexes ([positive cells/total cells] × 100) were calculated for each section. This was repeated twice to ensure that intraobserver variability was less than 10%. The area of the neointima and the media and adventitia for the venous anastomosis was determined by manually tracing the different layers of the vessel wall after immunostaining with hematoxylin-eosin. The neointima was defined as the area above the internal elastic lamina, which was easily determined from the media for three to five sections. The medial and adventitial area was defined from the internal elastic lamina to the fat surrounding the vessel wall.

TUNEL Staining

TUNEL staining was performed on paraffin-embedded sections from the outflow vein of MSC and control groups as specified by the manufacturer (Dead-End Colorimetric tunnel assay system, G7360; Promega, Madison, Wis). The negative control is shown where the recombinant terminal deoxynucleotidyl transferase enzyme was omitted.

RNA Isolation

The outflow vein was isolated and stored in RNA stabilizing reagent (Qiagen, Gaithersburg, Md) per the manufactures guidelines. To isolate the RNA, the specimens were homogenized, and total RNA from the samples was isolated by using the RNeasy Mini Kit (Qiagen) (25).

Real-time Polymerase Chain Reaction Analysis

Studies have demonstrated that MSCs exert their anti-inflammatory effect through a reduction in gene expression of *Mcp-1* (29). We assessed the gene expression of *Mcp-1* by performing real-time polymerase chain reaction analysis on day 7 after vessels with transplanted MSCs were compared with control AVFs alone. Expression for the gene of interest was determined by using real-time polymerase chain reaction analysis, as described previously (25). The primers used are shown in the Table.

Statistical Methods

Data are expressed as means ± standard errors of the mean. Multiple comparisons were performed with two-way analysis of variance, followed by the Student *t* test with post hoc Bonferroni correction. A significant difference from the control value was indicated by a *P* value less than .05. JMP version 9 software (SAS Institute, Cary, NC) was used for statistical analyses.

Mouse Primers Used

Gene	Sequence
Mcp-1	5′–GGAGAGCTACAAGAGGATCAC–3′ (sense)
	5′–TGATCTCATTTGGTTCCGATCC–3′ (antisense)
18S	5′–GTTCCGACCATAAACGATGCC-3′ (sense)
	5′-TGGTGGTGCCCTTCCGTCAAT-3′(antisense)

Results

Localization of MSCs after Adventitial Delivery to the Outflow Vein of AVF

MSCs were stably transfected with GFP so they could be identified after adventitial delivery by using confocal microscopy of the outflow vein, performed at different times. This demonstrated that GFP-positive cells from the vessels with transplanted MSCs (blue positive cells, Fig 1a) were present on day 7. However, by day 21, there was no visualization of the GFP signal (data not shown).

PET images of mice after adventitial delivery of ^{89}Zr-labeled MSCs showed that more than 90% of administered ^{89}Zr radioactivity was retained at the delivery site on day 4 (Fig 1). Adventitial retention of ^{89}Zr radioactivity cleared slowly from day 4 to day 21, losing approximately 20% over this period (Fig 1b). Most ^{89}Zr radioactivity that was cleared from the adventitia appeared to translocate to bones. This result confirmed the results obtained by using confocal microscopy with GFP-labeled cells on day 7. PET imaging of ^{89}Zr-labeled MSCs allowed tracking of cells beyond 7 days, which was not possible with GFP-labeled cells. The retention of most of the delivered stem cells at the delivery site on day 21 demonstrates that the effect is longer than what was visualized by using GFP labeling. In the case of the control group in which ^{89}Zr $(HPO_4)_2$ was administered, a biodistribution similar to that of ^{89}Zr-labeled MSCs was seen, with most of the radioactivity (approximately 80%) retained at the delivery site and the rest redistributing to bones.

Adventitial Transplantation of MSCs Reduces Gene Expression of *Mcp-1* at the Outflow Vein

The mean gene expression of *Mcp-1* at the outflow vein of vessels with transplanted MSCs was significantly lower than that in the control group (mean reduction, 62%; $P = .029$; Fig 2).

Adventitial Transplantation of MSCs to the Outflow Vein Reduces Mean Neointimal Area and Medial and Adventitial Area and Cell Density in the Neointima While Increasing Mean Lumen Vessel Area on Days 7 and 21

We determined the mean lumen vessel area on day 7 and observed that there was a significant increase in the outflow vein removed from vessels with transplanted MSCs versus the control group (mean increase, 176%; $P = .013$; Fig E3, *A* [online]). By day 21, it remained significantly increased in the vessels with transplanted MSCs when compared with the control group (mean increase, 415%; $P = .011$). We next determined the mean of the neointimal area and the medial and adventitial area. By day 21, there was a significant decrease in the neointimal area and the medial and adventitial area in the outflow vein removed from the vessels with transplanted MSCs when compared with the control group

Figure 1

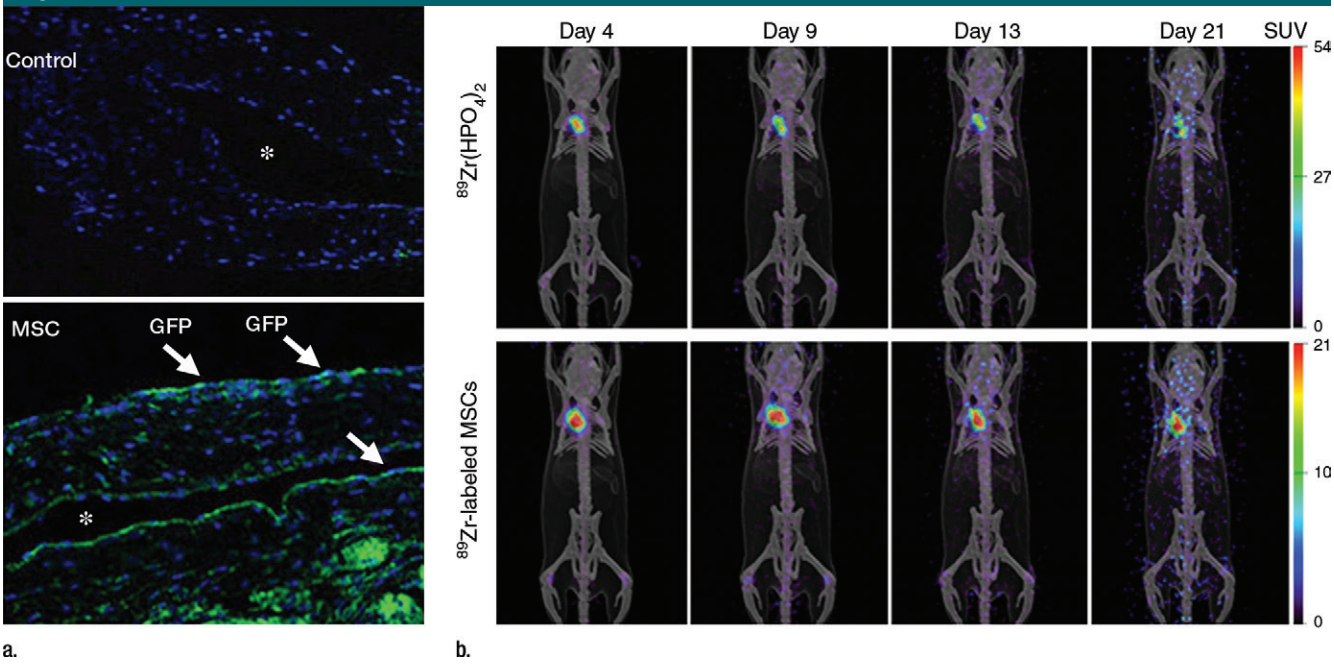

Figure 1: **(a)** Photomicrographs (original magnification, ×20) show the localization of human adipose tissue–derived MSCs. GFP was used to stably transfect 2.5 × 10^5 MSCs, which were injected into the adventitia of the outflow vein of the AVF at the time of creation. GFP-labeled human adipose tissue–derived MSCs are present on day 7 in vessels with transplanted MSCs compared with outflow vein vessels removed from control animals after AVF placement. Nuclei are blue. There are GFP-positive cells (arrows) in the vessel wall of the outflow vein on day 7. * = lumen. **(b)** Serial PET images of ^{89}Zr distribution in mice after adventitial delivery of ^{89}Zr-labeled MSCs or ^{89}Zr $(HPO_4)_2$. The anatomic reference skeleton images are formed by using the mouse atlas registration system algorithm with information obtained from the stationary top-view planar x-ray projector and side-view optical camera. *SUV* = standardized uptake value.

Figure 2

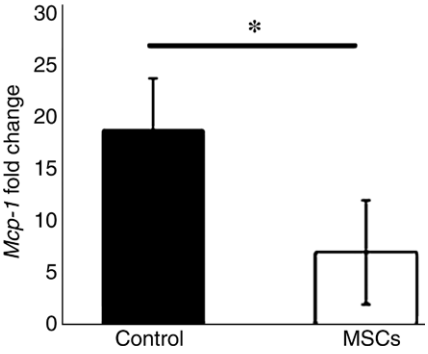

Figure 2: Graph shows *Mcp-1* gene expression on day 7 in vessels with transplanted MSCs compared with outflow vein vessels removed from control animals. There is a significant decrease in mean *Mcp-1* gene expression in the vessels with transplanted MSCs when compared with the control group ($P < .05$). Each bar shows the mean ± standard error of the mean of four to six animals per group. Two-way analysis of variance with the Student *t* test was performed. * = Significant ($P < .05$) differences among vessels with transplanted MSCs and control vessels.

(mean reduction, 77%; $P = .013$; Fig 3; Fig E3, *B* [online]).

By day 7, the mean cell density of the neointima in the MSC-treated vessels was significantly lower than that the control group (mean reduction, 83%; $P = .0007$; Fig E3, *C* [online]). By day 21, it remained lower in the vessels with transplanted MSCs when compared with the control group (mean reduction, 83%; $P < .0001$).

Adventitial Transplantation of MSCs to the Outflow Vein Increases TUNEL Staining

We speculated that the decrease in cell density was also due to an increase in apoptosis (30). Apoptosis was evaluated by using TUNEL staining (Fig 4, upper row). By day 7, the mean density of cells staining positive for TUNEL (brown-staining nuclei) at the outflow vein of vessels with transplanted MSCs was significantly increased compared with the control group (mean increase, 3061%; $P < .0001$). By day 21, it remained higher in the vessels with transplanted MSCs when compared with the control group (mean increase, 425%; $P < .0001$; Fig E4, *A* [online]). Therefore, these results demonstrate that vessels with transplanted MSCs have increased TUNEL activity, indicating cellular apoptosis when compared with control vessels.

Adventitial Transplantation of MSCs to the Outflow Vein Reduces Cellular Proliferation at the Outflow Vein

Because the cellular density was decreased, we determined if this was associated with a reduction in cellular proliferation that was assessed by using Ki-67 staining (brown-staining nuclei are positive for Ki-67; Fig 4, lower row). Seven days after fistula placement, there was a significant reduction in the mean Ki-67 index in the vessels

with transplanted MSCs when compared with the control group (mean reduction, 81%; P = .0003; Fig E4, *B* [online]). By day 21, it remained significantly lower in the vessels with transplanted MSCs when compared with the control vessels (mean reduction, 60%; P = .016).

Figure 3

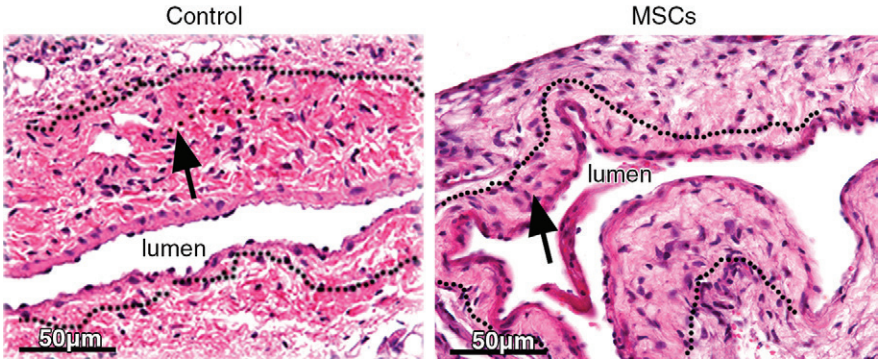

Figure 3: Photomicrographs (original magnification, ×40) show hematoxylin-eosin staining of vessels with transplanted MSCs (right) compared with outflow vein vessels removed from control animals with AVF only (left) on day 21 after placement. Arrows = neointima.

Adventitial Transplantation of MSCs to the Outflow Vein Reduces α-SMA and FSP-1 Staining

We assessed smooth-muscle deposition by using α-SMA staining (Fig 5, upper row). By day 21, the mean α-SMA staining was significantly lower in the vessels with transplanted MSCs when compared with the control group (mean reduction, 27%; P = .013; Fig E5, *A* [online]). FSP-1 has been used as a fibroblast marker (Fig 5, lower panel). In previous studies, investigators have demonstrated fibroblast to myofibroblast (α-SMA) differentiation, resulting in VNH (28,31). By day 7, we observed a significant decrease in the mean FSP-1 staining in the vessels with transplanted MSCs when compared with the control group (mean reduction, 65%; P = .0003; Fig E5, *B* [online]). By day 21, it remained significantly lower in the vessels with transplanted MSCs

Figure 4

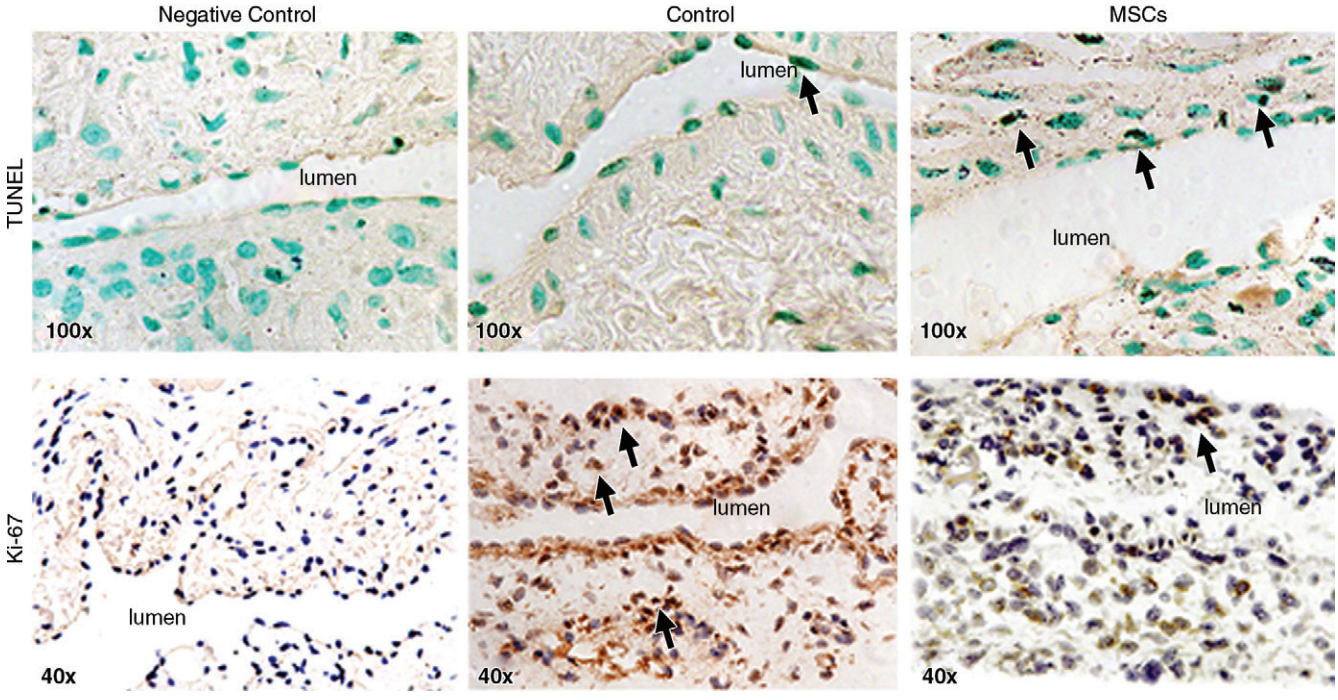

Figure 4: Photomicrographs (original magnification, ×100 [top row] and ×40 [bottom row]) show TUNEL and Ki-67 staining in murine AVF on day 7 after placement of AVF in the outflow vein alone (control animals) and in vessels with transplanted MSCs. The upper row is representative sections from TUNEL staining at the outflow vein of the vessels with transplanted MSCs and control vessels on day 7. Brown-staining nuclei are positive for TUNEL (arrows). The negative control is shown where the recombinant terminal deoxynucleotidyl transferase enzyme was omitted. The lower row is representative sections after Ki-67 staining in outflow vessels with transplanted MSCs or AVF alone in the control animals on day 7 after AVF placement. Brown-staining nuclei are positive for Ki-67. Negative controls stained with immunoglobulin G are shown.

Figure 5

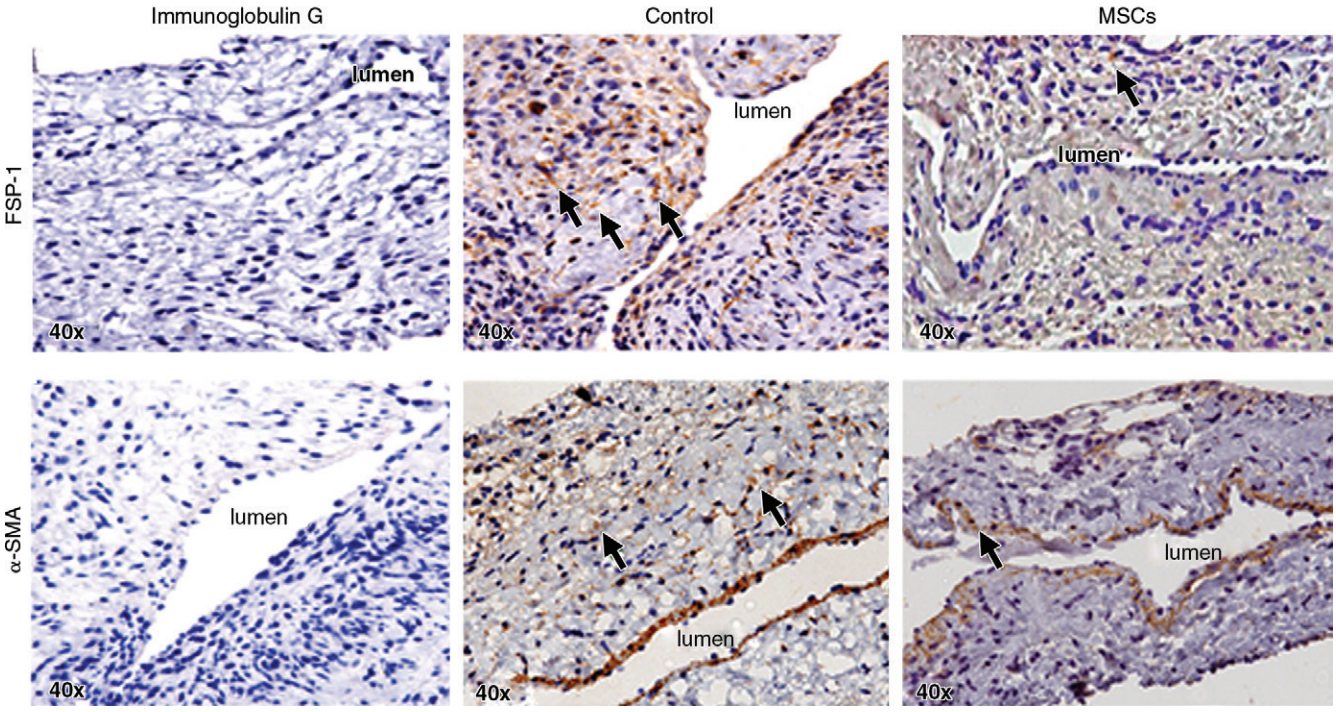

Figure 5: Photomicrographs (original magnification, ×40) show FSP-1 and α-SMA staining in murine AVF control animals on day 21 after placement of AVF in the outflow vein alone and vessels with transplanted MSCs. The upper row is the representative sections after FSP-1 staining in the venous stenosis of the vessels with transplanted MSCs and control vessels on day 21. Brown-staining cells are positive for FSP-1 (arrows). Negative controls stained with immunoglobulin G are shown. The lower row is the representative sections after α-SMA staining in the venous stenosis of the vessels with transplanted MSCs and control vessels on day 21. Brown-staining cells are positive for α-SMA (arrows).

when compared with the control group (mean reduction, 42%; P = .0016). Overall, these results indicate that on day 7, there is a reduction in FSP-1 staining, followed by a decrease in α-SMA staining by day 21 in vessels with transplanted MSCs when compared with control vessels.

Adventitial Transplantation of MSCs to the Outflow Vein Is Associated with a Reduction in HIF-1α Staining

We quantified HIF-1α staining to assess whether MSC transplantation had an effect on the expression of HIF-1α at the outflow vein of AVF. Brown-staining nuclei are positive for HIF-1α (Fig 6, upper row). By day 7, there was a significant reduction in the mean density of HIF-1α–staining vessels with transplanted MSCs when compared with control vessels (mean reduction, 67%; $P < .0001$; Fig E6, *A* [online]). By day 21, it remained significantly lower in the MSC-treated vessels when compared with control vessels (mean reduction, 62%; P = .0005). Overall, these results indicate that there is decreased expression in HIF-1α in vessels with transplanted MSCs when compared with control vessels.

Adventitial Transplantation of MSCs to the Outflow Vein Is Associated with a Reduction in CD68 Staining

Cells staining brown in the cytoplasm are positive for CD68 (Fig 6, lower row). By day 7, there was significant reduction in the mean density of CD68 staining in the MSC-treated vessels when compared with control vessels (mean reduction, 51%; P = .033; Fig E6, *B* [online]). Overall, there is a significant decrease in CD68 staining in the vessels with transplanted MSCs when compared with the control group.

Discussion

In our study, we demonstrated that adventitial transplantation of human adipose tissue–derived MSCs to the outflow vein of AVF in a murine model reduces VNH. This is mediated by a significant decrease in the gene expression of *Mcp-1* in the outflow vein with transplanted MSCs compared with the control group on day 7. There is a significant increase in mean TUNEL staining with a decrease in proliferation. Additionally, there is a significant decrease in FSP-1, CD68, and α-SMA staining, accompanied by a decrease in mean HIF-1α staining. Finally, Zr^{89}-labeled MSCs can be tracked up to 3 weeks after adventitial delivery.

Previous studies have shown that there is increased gene expression of *Mcp-1* at the AVF (5–7). Genetic deletion of Mcp-1 in experimental animal

Figure 6

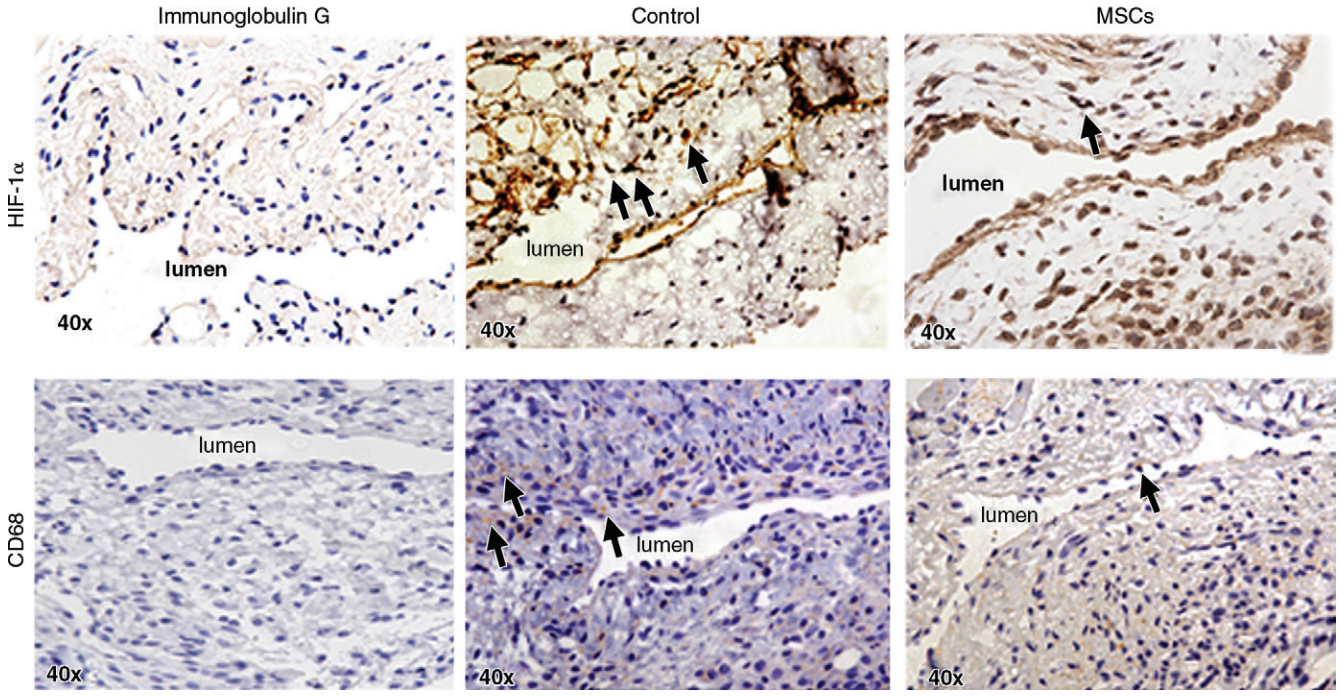

Figure 6: Photomicrographs (original magnification, ×40) show HIF-1α and CD68 staining in murine AVF on day 7 after placement in the outflow vein alone (control group) and vessels with transplanted MSCs. The upper row is the representative sections after HIF-1α staining in the venous stenosis of the vessels with transplanted MSCs and control vessels on day 7. Brown-staining nuclei are positive for HIF-1α staining. Negative controls stained with immunoglobulin G are shown. The lower row is the representative sections after CD68 staining in the venous stenosis of the vessels with transplanted MSCs and control vessels on day 7. Brown-staining cells are positive for CD68 staining.

models of AVF failure was associated with a reduction in venous stenosis formation (5). Mcp-1 was localized to the endothelium, smooth muscle cells, and leukocytes. In the present study, we observed that vessels with transplanted MSCs had reduced expression of Mcp-1, accompanied by a reduction in cells staining positive for FSP-1, α-SMA, and CD68. Adventitial transplantation of MSCs to the outflow vein at the time of AVF results in a reduction of several proinflammatory genes, including *Mcp-1*. Our findings are consistent with previous studies that have demonstrated that human MSC transplantation can reduce *Mcp-1* gene expression in experimental animal models of focal cerebral ischemia (32). Increased expression of the MCP-1/CCL2 axis is associated with the pathogenesis of several different fibrotic models involving the lung, kidney, and liver (33–36). Notably, *Mcp-1* is implicated in the dysfunction of AVF clinically and in experimental animal models (5,37). Studies conducted in patients with hemodialysis have shown that there are increased serum levels of MCP-1 and that this is considered to be a risk factor for AVF dysfunction (38,39).

VNH is characterized by an increase in cellular proliferation and extracellular matrix deposition and a decrease in apoptosis (8,40,41). Previous studies have demonstrated the inhibitory effects of MSC on proliferation of target cells, such as monocytes, tumor cells, and cardiac fibroblasts (17–20). Conversely, MSCs have been shown to induce proliferation and migration in lung fibroblasts and endothelial cells (42,43). Studies conducted at our laboratories and others have demonstrated that adventitial and medial fibroblasts can convert to myofibroblasts (α-SMA[+]) that can proliferate and migrate, leading to VNH formation (31,44).

In our study, we assessed cellular proliferation by performing Ki-67 staining and observed a significant reduction in cellular proliferation in vessels removed from animals with transplanted MSCs when compared with the control group. MSCs can exert an antiproliferative effect mediated in part by decreasing *Mcp-1* expression. Our finding is consistent with a study conducted in vitro in which CD14+ cells isolated from peripheral blood–enhanced fibroblast proliferation mediated through MCP-1 (45). In addition to reduced cellular proliferation, we also observed a significant decrease in cellular density, accompanied by a significant increase in TUNEL staining.

Hypoxic injury to the vessel wall of the outflow vein at the time of AVF placement and arterial bypass grafts can result in VNH (46–48). Several studies have demonstrated increased HIF-1α expression in animal models of hemodialysis graft failure and in clinical specimens from patients with hemodialysis vascular access failure (23,49–51). In our study, we found that adventitial transplantation of MSCs to adventitia of the outflow vein in a murine model results in a significant

reduction in the expression of HIF-1α. These findings indicate that MSC transplantation to the adventitia of the outflow vein is associated with a reduction in expression of HIF-1α, therefore possibly reducing hypoxia-induced inflammatory response in the vessel wall. It is well known that macrophages can home to areas of vascular injury associated with hypoxia, and we hypothesize that the reduction in HIF-1α and thus hypoxia is responsible for the decreased CD68 staining.

PET imaging of ^{89}Zr-labeled MSCs showed most (approximately 80%) of the radiolabel to be retained at the adventitial delivery site, even 3 weeks after delivery. This result confirms that the cells are in contact with the adventitia of the outflow vein for a prolonged period after delivery. The similar imaging findings with ^{89}Zr $(HPO_4)_2$, which delivered ^{89}Zr in its "free" cationic form to the adventitia, would appear to indicate that the adventitia is not well perfused. Thus, the slow release of ^{89}Zr-labeled MSCs from the adventitia cannot be interpreted as strong evidence of specific binding of the cells to the adventitia. In contrast, ^{89}Zr-labeled MSCs delivered intravenously home to the lung, followed by the liver and bones, and free ^{89}Zr $(HPO_4)_2$ is mainly localized in the liver and bones. These differences in biodistribution provide further evidence that the prolonged retention of both ^{89}Zr-labeled MSCs and ^{89}Zr $(HPO_4)_2$ may be explained by the lack of perfusion on the surface of the adventitia due to a less defined vasa vasorum surrounding the vein when compared with the artery (20). Additionally, the use of ^{89}Zr-labeled MSCs was more sensitive than GFP labeling for detection of cellular location after delivery.

There are several limitations to our study. We used an immunodeficient mouse, and a potential T cell–mediated mechanism involved in the pathophysiology of VNH could not be evaluated. A murine model of normal kidney function was used; thus, the effects of chronic kidney disease could not be evaluated. Finally, these results need to be corroborated by using larger animal models, as the murine model may not simulate the clinical scenario.

In conclusion, we demonstrate that adventitial transplantation of human adipose tissue–derived MSCs to the outflow vein of a murine model of AVF results in a decrease in the gene expression of *Mcp-1*. This resulted in a reduction in VNH, accompanied by a decrease in cell proliferation and an increase in apoptosis with positive vascular remodeling. The clinical importance of this study is that it provides a rationale for using MSC transplantation in patients with hemodialysis AVF access for reducing VNH and highlights the fact that MSCs can be tracked after delivery by using PET imaging of ^{89}Zr-labeled MSCs.

Acknowledgments: The authors thank Jay Mandrekar, PhD, for his biostatistical expertise in interpreting the results.

Disclosures of Conflicts of Interest: B.Y. disclosed no relevant relationships. **A. Brahmbhatt** disclosed no relevant relationships. **E.N.T.** disclosed no relevant relationships. **B.T.** disclosed no relevant relationships. **D.L.M.** disclosed no relevant relationships. **S.E.** disclosed no relevant relationships. **A. Bansal** disclosed no relevant relationships. **M.K.P.** disclosed no relevant relationships. **A.B.D.** Activities related to the present article: disclosed no relevant relationships. Activities not related to the present article: author is an inventor of technology at Mill Creek Life Sciences, which supplies technology for growing MSCs, and has a leadership position within the company. Other relationships: author has a patent pending for methods and materials for reducing VNH of an AVF or graft. **E.B.L.** disclosed no relevant relationships. **T.R.D.** Activities related to the present article: disclosed no relevant relationships. Activities not related to the present article: disclosed no relevant relationships. Other relationships: author has a patent pending for ^{89}Zr-labeled cells. **D.M.** disclosed no relevant relationships. **S.M.** Activities related to the present article: disclosed no relevant relationships. Activities not related to the present article: disclosed no relevant relationships. Other relationships: author has a patent pending for preventing venous stenosis formation with MSCs.

References

1. Collins AJ, Foley RN, Chavers B, et al. US Renal Data System 2013 Annual Data Report. Am J Kidney Dis 2014;63(1 Suppl):A7.
2. Roy-Chaudhury P, Kelly BS, Zhang J, et al. Hemodialysis vascular access dysfunction: from pathophysiology to novel therapies. Blood Purif 2003;21(1):99–110.
3. Rotmans JI, Pasterkamp G, Verhagen HJ, Pattynama PM, Blankestijn PJ, Stroes ES. Hemodialysis access graft failure: time to revisit an unmet clinical need? J Nephrol 2005;18(1):9–20.
4. Riella MC, Roy-Chaudhury P. Vascular access in haemodialysis: strengthening the Achilles' heel. Nat Rev Nephrol 2013;9(6):348–357.
5. Juncos JP, Grande JP, Kang L, et al. MCP-1 contributes to arteriovenous fistula failure. J Am Soc Nephrol 2011;22(1):43–48.
6. Mattana J, Effiong C, Kapasi A, Singhal PC. Leukocyte-polytetrafluoroethylene interaction enhances proliferation of vascular smooth muscle cells via tumor necrosis factor-alpha secretion. Kidney Int 1997;52(6):1478–1485.
7. Dukkipati R, Molnar MZ, Park J, et al. Association of vascular access type with inflammatory marker levels in maintenance hemodialysis patients. Semin Dial 2014;27(4):415–423.
8. Roy-Chaudhury P, Kelly BS, Miller MA, et al. Venous neointimal hyperplasia in polytetrafluoroethylene dialysis grafts. Kidney Int 2001;59(6):2325–2334.
9. Pittenger MF, Mackay AM, Beck SC, et al. Multilineage potential of adult human mesenchymal stem cells. Science 1999;284(5411):143–147.
10. Prockop DJ, Olson SD. Clinical trials with adult stem/progenitor cells for tissue repair: let's not overlook some essential precautions. Blood 2007;109(8):3147–3151.
11. Oyagi S, Hirose M, Kojima M, et al. Therapeutic effect of transplanting HGF-treated bone marrow mesenchymal cells into CCl4-injured rats. J Hepatol 2006;44(4):742–748.
12. Abdel Aziz MT, Atta HM, Mahfouz S, et al. Therapeutic potential of bone marrow–derived mesenchymal stem cells on experimental liver fibrosis. Clin Biochem 2007;40(12):893–899.
13. Nagaya N, Kangawa K, Itoh T, et al. Transplantation of mesenchymal stem cells improves cardiac function in a rat model of dilated cardiomyopathy. Circulation 2005;112(8):1128–1135.
14. Ortiz LA, Gambelli F, McBride C, et al. Mesenchymal stem cell engraftment in lung is enhanced in response to bleomycin exposure and ameliorates its fibrotic effects. Proc Natl Acad Sci U S A 2003;100(14):8407–8411.
15. Ninichuk V, Gross O, Segerer S, et al. Multipotent mesenchymal stem cells reduce interstitial fibrosis but do not delay progression of chronic kidney disease in collagen4A3-deficient mice. Kidney Int 2006;70(1):121–129.
16. Caplan AI. Why are MSCs therapeutic? New data: new insight. J Pathol 2009;217(2):318–324.

17. Ramasamy R, Fazekasova H, Lam EW, Soeiro I, Lombardi G, Dazzi F. Mesenchymal stem cells inhibit dendritic cell differentiation and function by preventing entry into the cell cycle. Transplantation 2007;83(1):71–76.

18. Ramasamy R, Lam EW, Soeiro I, Tisato V, Bonnet D, Dazzi F. Mesenchymal stem cells inhibit proliferation and apoptosis of tumor cells: impact on in vivo tumor growth. Leukemia 2007;21(2):304–310.

19. Li L, Zhang S, Zhang Y, Yu B, Xu Y, Guan Z. Paracrine action mediate the antifibrotic effect of transplanted mesenchymal stem cells in a rat model of global heart failure. Mol Biol Rep 2009;36(4):725–731.

20. Ohnishi S, Sumiyoshi H, Kitamura S, Nagaya N. Mesenchymal stem cells attenuate cardiac fibroblast proliferation and collagen synthesis through paracrine actions. FEBS Lett 2007;581(21):3961–3966.

21. Das R, Jahr H, van Osch GJ, Farrell E. The role of hypoxia in bone marrow–derived mesenchymal stem cells: considerations for regenerative medicine approaches. Tissue Eng Part B Rev 2010;16(2):159–168.

22. Hu X, Yu SP, Fraser JL, et al. Transplantation of hypoxia-preconditioned mesenchymal stem cells improves infarcted heart function via enhanced survival of implanted cells and angiogenesis. J Thorac Cardiovasc Surg 2008;135(4):799–808.

23. Misra S, Shergill U, Yang B, Janardhanan R, Misra KD. Increased expression of HIF-1α, VEGF-A and its receptors, MMP-2, TIMP-1, and ADAMTS-1 at the venous stenosis of arteriovenous fistula in a mouse model with renal insufficiency. J Vasc Interv Radiol 2010;21(8):1255–1261.

24. Das M, Burns N, Wilson SJ, Zawada WM, Stenmark KR. Hypoxia exposure induces the emergence of fibroblasts lacking replication repressor signals of PKCζ in the pulmonary artery adventitia. Cardiovasc Res 2008;78(3):440–448.

25. Yang B, Shergill U, Fu AA, Knudsen B, Misra S. The mouse arteriovenous fistula model. J Vasc Interv Radiol 2009;20(7):946–950.

26. Crespo-Diaz R, Behfar A, Butler GW, et al. Platelet lysate consisting of a natural repair proteome supports human mesenchymal stem cell proliferation and chromosomal stability. Cell Transplant 2011;20(6):797–811.

27. Bansal A, Pandey MK, Demirhan YE, et al. Novel (89)Zr cell labeling approach for PET-based cell trafficking studies. EJNMMI Res 2015;5:19.

28. Misra S, Doherty MG, Woodrum D, et al. Adventitial remodeling with increased matrix metalloproteinase-2 activity in a porcine arteriovenous polytetrafluoroethylene grafts. Kidney Int 2005;68(6):2890–2900.

29. Wise AF, Williams TM, Kiewiet MB, et al. Human mesenchymal stem cells alter macrophage phenotype and promote regeneration via homing to the kidney following ischemia-reperfusion injury. Am J Physiol Renal Physiol 2014;306(10):F1222–F1235.

30. Shay-Salit A, Shushy M, Wolfovitz E, et al. VEGF receptor 2 and the adherens junction as a mechanical transducer in vascular endothelial cells. Proc Natl Acad Sci U S A 2002;99(14):9462–9467.

31. Wang Y, Krishnamoorthy M, Banerjee R, et al. Venous stenosis in a pig arteriovenous fistula model—anatomy, mechanisms and cellular phenotypes. Nephrol Dial Transplant 2008;23(2):525–533.

32. Wang H, Nagai A, Sheikh AM, et al. Human mesenchymal stem cell transplantation changes proinflammatory gene expression through a nuclear factor-κB–dependent pathway in a rat focal cerebral ischemic model. J Neurosci Res 2013;91(11):1440–1449.

33. Hartl D, Griese M, Nicolai T, et al. A role for MCP-1/CCR2 in interstitial lung disease in children. Respir Res 2005;6:93.

34. Okuma T, Terasaki Y, Kaikita K, et al. C-C chemokine receptor 2 (CCR2) deficiency improves bleomycin-induced pulmonary fibrosis by attenuation of both macrophage infiltration and production of macrophage-derived matrix metalloproteinases. J Pathol 2004;204(5):594–604.

35. Tesch GH. MCP-1/CCL2: a new diagnostic marker and therapeutic target for progressive renal injury in diabetic nephropathy. Am J Physiol Renal Physiol 2008;294(4):F697–F701.

36. Kanno K, Tazuma S, Nishioka T, Hyogo H, Chayama K. Angiotensin II participates in hepatic inflammation and fibrosis through MCP-1 expression. Dig Dis Sci 2005;50(5):942–948.

37. Liu BC, Li L, Gao M, Wang YL, Yu JR. Microinflammation is involved in the dysfunction of arteriovenous fistula in patients with maintenance hemodialysis. Chin Med J (Engl) 2008;121(21):2157–2161.

38. Papayianni A, Alexopoulos E, Giamalis P, et al. Circulating levels of ICAM-1, VCAM-1, and MCP-1 are increased in haemodialysis patients: association with inflammation, dyslipidaemia, and vascular events. Nephrol Dial Transplant 2002;17(3):435–441.

39. De Marchi S, Falleti E, Giacomello R, et al. Risk factors for vascular disease and arteriovenous fistula dysfunction in hemodialysis patients. J Am Soc Nephrol 1996;7(8):1169–1177.

40. Swedberg SH, Brown BG, Sigley R, Wight TN, Gordon D, Nicholls SC. Intimal fibromuscular hyperplasia at the venous anastomosis of PTFE grafts in hemodialysis patients. Clinical, immunocytochemical, light and electron microscopic assessment. Circulation 1989;80(6):1726–1736.

41. Rekhter M, Nicholls S, Ferguson M, Gordon D. Cell proliferation in human arteriovenous fistulas used for hemodialysis. Arterioscler Thromb 1993;13(4):609–617.

42. Salazar KD, Lankford SM, Brody AR. Mesenchymal stem cells produce Wnt isoforms and TGF-β1 that mediate proliferation and procollagen expression by lung fibroblasts. Am J Physiol Lung Cell Mol Physiol 2009;297(5):L1002–L1011.

43. Potapova IA, Gaudette GR, Brink PR, et al. Mesenchymal stem cells support migration, extracellular matrix invasion, proliferation, and survival of endothelial cells in vitro. Stem Cells 2007;25(7):1761–1768.

44. Li L, Terry CM, Blumenthal DK, et al. Cellular and morphological changes during neointimal hyperplasia development in a porcine arteriovenous graft model. Nephrol Dial Transplant 2007;22(11):3139–3146.

45. Liao WT, Yu HS, Arbiser JL, et al. Enhanced MCP-1 release by keloid CD14+ cells augments fibroblast proliferation: role of MCP-1 and Akt pathway in keloids. Exp Dermatol 2010;19(8):e142–e150.

46. Lata C, Green D, Wan J, Roy S, Santilli SM. The role of short-term oxygen administration in the prevention of intimal hyperplasia. J Vasc Surg 2013;58(2):452–459.

47. Lee ES, Bauer GE, Caldwell MP, Santilli SM. Association of artery wall hypoxia and cellular proliferation at a vascular anastomosis. J Surg Res 2000;91(1):32–37.

48. Santilli SM, Wernsing SE, Lee ES. Transarterial wall oxygen gradients at a prosthetic vascular graft to artery anastomosis in the rabbit. J Vasc Surg 2000;31(6):1229–1239.

49. Misra S, Fu AA, Rajan DK, et al. Expression of hypoxia inducible factor-1α, macrophage migration inhibition factor, matrix metalloproteinase-2 and -9, and their inhibitors in hemodialysis grafts and arteriovenous fistulas. J Vasc Interv Radiol 2008;19(2 Pt 1):252–259.

50. Yang B, Janardhanan R, Vohra P, et al. Adventitial transduction of lentivirus-shRNA-VEGF-A in arteriovenous fistula reduces venous stenosis formation. Kidney Int 2014;85(2):289–306.

51. Janardhanan R, Yang B, Vohra P, et al. Simvastatin reduces venous stenosis formation in a murine hemodialysis vascular access model. Kidney Int 2013;84(2):338–352.